Breast Deformation in Near Infrared Optical Tomography

Hamid Dehghani[1], Brian W. Pogue[1], Marvin M. Doyley[2], Jason Geng[3] and Keith D. Paulsen[1]
[1]*Thayer School of Engineering, Dartmouth College, Hanover, NH 03755*
[2]*Department of Radiology, Dartmouth Medical School, Hanover, NH 03755*
[3]*Genex Technologies, Inc. 10605 Concord Street, Suite 500, Kensington, MD 20895-2504*
email:dehghani@dartmouth.edu, Tel:(603) 646-9193, Fax:(603) 646-3856

Abstract: In NIR tomography of the breast, good contact is needed by the fibers, resulting in breast deformation. We present a deformation model to account for the change of shape and discuss implications in image reconstruction.

OCIS codes: (170.3830) Mammography; (170.6960) Tomography; (100.3010) Image reconstruction techniques; (100.3190) Inverse problems

1. Introduction

Near Infrared (NIR) tomography is an emerging alternative imaging method used to image physiologic parameters of biological tissue in-vivo such as water and hemoglobin [1]. Measurements of light propagation (600 – 900 nm) within tissue can be used to map internal chromophore concentrations within tissue. Light is transmitted through tissue using multiple input and output locations on the surface of the region to be imaged using optical fibers for delivery and pickup of the light signals. To obtain clinical measurements with a sufficient signal to noise ratio, it is key to ensure good contact exists between the optical fibers and the tissue. The breast is a soft tissue, which will deform and alter its shape on the application of external pressure. The amount of deformation is a function of the tissue mechanical properties and the amount of displacement and the external pressure applied by the optical fiber array. In most image reconstruction algorithms, the general assumption is made that the region under investigation is a uniform circular (2D) or conical or cylindrical (3D) domain [2]. Little work has been done to evaluate the effect of any incorrect geometry in image reconstruction. In this work, the effect of such assumptions is investigated by creating a deformation of the breast model in 3D to generate stimulated clinical data. Images are then reconstructed using various assumptions regarding the imaging domain such as 3D conical shaped models and the non-deformed breast model to evaluate image quality.

2. Methods

Soft tissues exhibit nonlinear elastic behavior. Nevertheless, they can be considered a linear elastic material in situations where the deforming forces produce infinitesimal deformations (i.e. ≤ 5 %). For the purpose of this study, the breast was modeled as linear isotropic pseudo-incompressible medium (i.e. Poisson's ratio (ν)= 0.495). Under these assumptions and ignoring internal body force, the governing elasticity equations for quasi-static deformation is given by:

$$(\lambda+\mu)\nabla(\nabla\cdot\vec{u})+\mu\nabla^2\vec{u}=0 \qquad \text{for internal nodes in domain } \mathbf{\Omega} \qquad (1)$$

$$\left((\lambda+\mu)\nabla(\nabla\cdot\vec{u})+\mu\nabla^2\vec{u}\right)\hat{n}=h \qquad \text{for nodes on the boundary } \delta\mathbf{\Omega}. \qquad (2)$$

Here $\hat{n}$ represents a unit vector directed outwards from Ω, and *h* represents the traction on the surface or boundary of the breast. Note that $\vec{u}$ represents the displacement components in all coordinate directions, and μ and λ are Lame's elastic constants. For an isotropic medium these constants are related to the more familiar Young's modulus (E) and the Poisson's ratio (ν) by $\mu=\frac{E}{2(1+\nu)}$ and $\lambda=\frac{\nu E}{(1+\nu)(1-2\nu)}$.

It should be stated that in this study the breast was assumed to be traction free and internal body forces were neglected, thus the problem was solved by imposing a prescribed displacement [3]. A volume mesh of a female breast of a volunteer was created from surface image data that was acquired using a 3D surface camera [Rainbow 3D Camera, Genex Technologies, Kensington MD]. The 3D camera projects structural illumination patterns onto the object and calculates 3D surface profile described by over 300,000 data points [4]. A volume mesh was then generated using the Delaunay algorithm**.** The mesh has a geometry of 130 x 136 x 60 mm, Figure 1(a) and contained 15501 nodes corresponding to 61171 linear tetrahedral elements. The diameter of the breast at its mid-plane where

optical fiber array would be applied is approximately 88 mm. To calculate the deformation due to 16 equally spaced optical fibers being applied at the mid-plane of the breast, i.e. z = -30 mm, it is assumed that each optical fiber pushed the breast so that the final breast diameter at z = -30 mm is 70 mm, and that the diameter of each optical fiber is 6 mm. The modeled elastic properties of tissue, were assumed as isotropic and homogenous with Young's Modulus of 20 kPa and Poisson's ratio of 0.495. Further, it was assumed that the top most part of the mesh, i.e. z = 0 mm was not allowed to move since it is connected to the chest. Using this applied displacement as a boundary condition, the displacement at all nodes due to the application of the optical fibers was calculated and a deformed mesh was created, Figure 1(b).

Figure 1. Volume mesh is shown of the (a) normal suspended breast and (b) the deformed mesh after the application of the optical fiber array.

In order to accurately simulate the clinical settings, two localized anomaly regions were placed within the mid-plane of the normal breast, both at z = -30 mm, Figure 2(a). First was an absorbing anomaly, 19 mm from the surface and a radius 10 mm with a coefficient value of 0.03 mm^{-1}. Second was a reduced scattering anomaly, also 19 mm from the surface but with a radius of 7.5 mm and a value of 3 mm^{-1}. The background optical properties were modeled with an absorption coefficient of 0.01 mm^{-1} and a reduced scatter coefficient of 1.0 mm^{-1}. For the deformed breast model the same optical properties of the normal breast, including the anomalies were assumed. Once the deformation of the model was calculated, it was assumed that the anomalies were free to move, depending on the elastic properties of the breast, Figure 2(b).

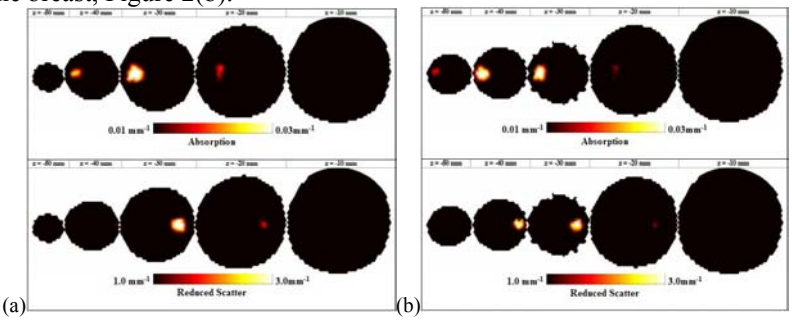

Figure 2. 2D coronal slices through (a) the normal breast mesh and (b) the deformed breast mesh, showing the position of the anomalies. The right hand slice is near the chest while the most left hand slice is near the nipple.

Using the deformed mesh, together with the displaced anomalies, NIR data were simulated for 16 equally circularly spaced optical fibers placed at z = -30 mm. Amplitude and phase data were simulated at 100 MHz, and 1% noise were added. This data was then used as simulated patient data in the following sections. In addition, to allow data calibration as done using clinical data, and discussed elsewhere [2], the data was simulated for 16 equally spaced optical fibers placed in a circle around the mid-plane of a cylindrical model with homogenous background optical properties.

3. Results

Assuming that correct anatomical information regarding the breast is available, before application of the optical fiber array, the normal, non-deformed mesh was used, Figure 1(a), during reconstruction to produce the images shown in Figure 3(a). Also, images reconstructed assuming a conical shaped breast (diameter at z = -30 set to equal the diameter of the optical fiber array) are shown in Figure 3(b). Finally, to show the best possible reconstruction, the deformed mesh was used for reconstruction of images and these results are shown in Figure 3(c).

From images reconstructed using the correct but non-deformed breast, although the absorbing anomaly has been recovered, the reduced scattering images contain large artifacts. The background absorption and scatter values are about 0.006 mm^{-1} and 0.5 mm^{-1} respectively, while the maximum absorption for the anomaly is 0.014 mm^{-1}. In images assuming a conical model the background absorption and scatter values are about 0.007 mm^{-1} and 0.94 mm^{-1}

respectively, while the maximum absorption for the anomaly is 0.014 mm^{-1}. Here, although the target values are better quantitatively, the images contain artifacts, are much smaller, and the absorption scatter cross-talk is more than expected. In images reconstructed assuming correct 3D deformed boundary, both the absorbing and scattering regions have been recovered with improved localization accuracy. Some cross talk exists between the absorbing and scattering anomalies. The background absorption and scatter values are about 0.01 mm^{-1} and 0.98 mm^{-1} respectively, while the maximum absorption and scatter values for the anomalies are 0.013 mm^{-1} and 1.3 mm^{-1} respectively. It is important to note that although the images in Figure 3(a) show a better quantitative accuracy for the recovered absorbing anomalies, the background values are much lower than expected and the images contain far more artifacts.

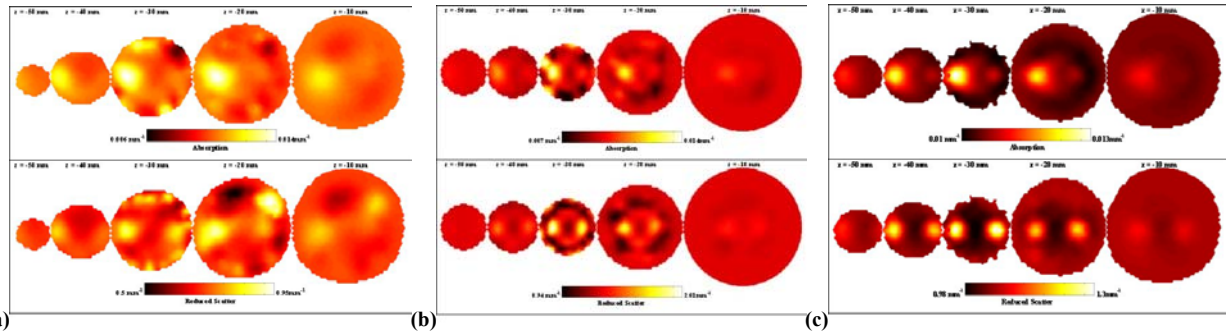

(a) (b) (c)

Figure 3. 3D simultaneous reconstruction of absorption and reduced scatter from deformed breast model simulated data are shown. The mesh used for the reconstruction was (a) the normal un-deformed breast; (b) conical mesh and (c) the correct deformed breast. The most right hand slice is near the chest while the most left hand slice is near the nipple in each set of images.

4. Discussion

In the case where it is assumed that the exact breast geometry is known, but the details of the fibers compression have been ignored, although the absorption anomaly was recovered with relatively good accuracy, the reduced scattering image contains a large artifact. Furthermore, the calculated background values for absorption and scatter are 0.006mm^{-1} and 0.5 mm^{-1} respectively, which are much lower than expected. These images are, perhaps, not as accurate and useful as the conical geometry case, since, although there is a more accurate 3D model, the diameter of the breast was not correct, particularly within the measurement plane, i.e. z = -30 mm. When using the geometrically correct deformed mesh to reconstruct images of absorption and scatter, superior localization accuracy resulted. The scattering object has also been recovered in this case. However, the quantitative accuracy of the recovered anomalies is not as good with maximum values for absorption and scatter of 0.013mm^{-1} and 1.3 mm^{-1}, respectively. This modest degradation in quantitative accuracy has been reported elsewhere and is a common problem in 3D imaging algorithms, which may be solved through the use of multi-stage algorithms [5] or with inclusion of a priori data. Nonetheless using the correct model with correct information regarding the deformed boundary has produced images with very little to no artifacts.

5. Acknowledgements

This work has been sponsored by the National Cancer Institute through grants RO1CA69544 and PO1CA80139 as well as DOD Breast cancer research program DAMD17-03-01-0405.

6. References

1. McBride, T.O., Pogue B W , S. Jiang, U. L. Osterberg, K. D. Paulsen, and S. P. Poplack, *Multi-spectral near-infrared tomography: a case study in compensating for water and lipid content in hemoglobin imaging of the breast.* J. Biomed. Opt., 2002. **7**.
2. Dehghani, H., Pogue, B. W., Poplack, S. P., Paulsen, K. D., *Multiwavelength Three-Dimensional Near-Infrared Tomography of the Breast: Initial Simulation, Phantom, and Clinical Results.* Applied Optics, 2003. **42**(1): p. 135-145.
3. Doyley, M.M., Meaney, P. M., and Bamber, J. C., *Evaluation of an iterative reconstruction method for quantitative elastography.* Phys. Med. Biol., 2000. **45**(6): p. 1521-1540.
4. Geng, Z., *Rainbow 3D Camera - A New Concept for High Speed and Low-Cost 3D Vision.* Journal Optical Engineering, 1996. **35**(2): p. 376.
5. Srinivasan, S., Pogue, B. W., Dehghani, H., Jiang, S., Song, X., and Paulsen, K. D., *Improved Quantification of Small Objects in Near-Infrared Diffuse Optical Tomography.* J. Biomed. Opt., 2003. **Submitted**.